

Exploring Alternative Synthetic Routes for the Preparation of Five-Coordinate Diamidoamine Group 4 Metal Complexes

Alicia R. Morgan,^{1a} Michael Kloskowski,^{1b} Felix Kalischewski,^{1b}
Aaron H. Phillips,^{1a} and Jeffrey L. Petersen^{*,1a}

*C. Eugene Bennett Department of Chemistry, West Virginia University,
Morgantown, West Virginia 26506-6045*

Received June 16, 2005

Efficient synthetic routes for the preparation of electrophilic titanium and zirconium complexes featuring a tridentate diamidoamine ligand have been developed. The five-coordinate titanium dichloride complexes [(MesNCH₂CH₂)₂NR]TiCl₂ (R = H (**3**), SiMe₃ (**4**)) are conveniently prepared from the amine elimination reactions of the triamines (MesNHCH₂CH₂)₂NR (R = H (**1**), SiMe₃ (**2**)) with Ti(NEt₂)₂Cl₂. Treatment of Ti(NEt₂)₄ with 2 equiv of SiMe₃Cl offers an effective method for the preparation of Ti(NEt₂)₂Cl₂. The corresponding five-coordinate zirconium homologues [(MesNCH₂CH₂)₂NR]ZrCl₂ (R = H (**5**), SiMe₃ (**6**)) are synthesized via the toluene elimination reactions of Zr(benzyl)₂Cl₂(Et₂O)₂ with **1** and **2**, respectively. The thermally unstable and photosensitive Zr(benzyl)₂Cl₂(Et₂O)₂ species may be prepared in situ from the reaction of Zr(benzyl)₄ with 2 equiv of [NEt₃H]Cl in diethyl ether at 0 °C in the dark. The toluene elimination reaction of Hf(benzyl)₄ with **1** affords the dibenzyl Hf complex [(MesNCH₂CH₂)₂NH]Hf(benzyl)₂, **7**. The X-ray structural and solution NMR data for **4**, **5**, **6**, and **7** reveal that these electrophilic group 4 metal complexes adopt the facial structure with either a chloride or a η²-benzyl ligand trans to the central amino N atom of the tridentate diamidoamine ligand.

Introduction

Electrophilic early transition metal complexes featuring multifunctional ligands have provided a new generation of “non-metallocene” catalysts for olefin polymerization.² The use of a chelating diamido ligand has led to the preparation of four- and five-coordinate precursors capable of promoting the living polymerization of α-olefins. McConville and co-workers^{3,4} observed that four-coordinate titanium dialkyl complexes derived from [ArN(CH₂)₃NAr]TiCl₂, where Ar = 2,6-ⁱPr₂C₆H₃ and 2,6-Me₂C₆H₃, when activated with MAO, B(C₆F₅)₃, or [Ph₃C][B(C₆F₅)₄], catalyze the polymerization of 1-hexene. The [ArN(CH₂)₃NAr]TiCl₂ complexes were prepared by the elimination of 2 equiv of SiMe₃Cl from the reactions of the corresponding silylated diamines Ar(SiMe₃)N(CH₂)₃N(SiMe₃)Ar with TiCl₄.

During the past decade Schrock and his colleagues have systematically explored the use of tridentate diamido ligands featuring a neutral N (pyridyl^{5–8} or

amine^{9–12}), O (diaryl ether^{13–16} or dialkyl ether^{17–19}), or S (diaryl thioether²⁰ or dialkyl thioether¹⁸) donor to prepare a myriad of five-coordinate metal complexes as catalyst precursors. They observed that [(MesNCH₂CH₂)₂NMe]ZrMe₂,^{9,10} when activated with [Ph₃C][B(C₆F₅)₄], promotes the polymerization of 1-hexene at 0–20 °C. Although this catalyst system was nearly living in terms of β-hydrogen elimination, the activity decreases at a moderate rate due to intramolecular cyclometalation

(7) Mehrkhodavandi, P.; Schrock, R. R.; Bonitatebus, P. J., Jr. *Organometallics* **2002**, *21*, 5785–5798.

(8) Schrock, R. R.; Adamchuk, J.; Ruhland, K.; Lopez, L. P. H. *Organometallics* **2003**, *22*, 5079–5091.

(9) Liang, L.-C.; Schrock, R. R.; Davis, W. M.; McConville, D. H. *J. Am. Chem. Soc.* **1999**, *121*, 5797–5798.

(10) Schrock, R. R.; Casado, A. L.; Goodman, J. T.; Liang, L.-C.; Bonitatebus, P. J., Jr.; Davis, W. M. *Organometallics* **2000**, *19*, 5325–5341.

(11) Schrock, R. R.; Bonitatebus, P. J., Jr.; Schrodi, Y. *Organometallics* **2001**, *20*, 1056–1058.

(12) Schrodi, Y.; Schrock, R. R.; Bonitatebus, P. J., Jr. *Organometallics* **2001**, *20*, 3560–3573.

(13) Baumann, R.; Davis, W. M.; Schrock, R. R. *J. Am. Chem. Soc.* **1997**, *119*, 3830–3831.

(14) Schrock, R. R.; Baumann, R.; Reid, S. M.; Goodman, J. T.; Stumpf, R.; Davis, W. M. *Organometallics* **1999**, *18*, 3649–3670.

(15) Baumann, R.; Stumpf, R.; Davis, W. M.; Liang, L.-C.; Schrock, R. R. *J. Am. Chem. Soc.* **1999**, *121*, 7822–7836.

(16) Liang, L.-C.; Schrock, R. R.; Davis, W. M. *Organometallics* **2000**, *19*, 2526–2531.

(17) Schrock, R. R.; Schattenmann, F.; Aizenberg, M.; Davis, W. M. *Chem. Commun.* **1998**, 199–200.

(18) Aizenberg, M.; Turculet, L.; Davis, W. M.; Schattenmann, F.; Schrock, R. R. *Organometallics* **1998**, *17*, 4795–4812.

(19) Flores, M. A.; Manzoni, M. R.; Baumann, R.; Davis, W. M.; Schrock, R. R. *Organometallics* **1999**, *18*, 3220–3227.

(20) Graf, D. G.; Schrock, R. R.; Davis, W. M.; Stumpf, R. *Organometallics* **1999**, *18*, 843–852.

* To whom correspondence should be addressed. E-mail: jpeterse@wvu.edu.

(1) (a) West Virginia University. (b) Visiting student, University of Münster.

(2) Gibson, V. C.; Spitzmesser, S. K. *Chem. Rev.* **2003**, *103*, 283–315.

(3) Scollard, J. D.; McConville, D. H. *J. Am. Chem. Soc.* **1996**, *118*, 10008–10009.

(4) Scollard, J. D.; McConville, D. H.; Payne, N. C.; Vittal, J. J. *Macromolecules* **1996**, *29*, 5241–5243.

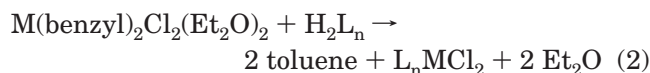
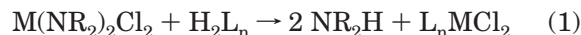
(5) Mehrkhodavandi, P.; Bonitatebus, P. J., Jr.; Schrock, R. R. *J. Am. Chem. Soc.* **2000**, *122*, 7841–7842.

(6) Mehrkhodavandi, P.; Schrock, R. R. *J. Am. Chem. Soc.* **2001**, *123*, 10746–10747.

that leads to dimerization^{10–12} and deactivation. When the *ortho*-methyl groups of the aryl substituents were replaced with chlorine atoms, the resultant system performed as a living catalyst for 1-hexene polymerization with no evidence of catalyst decomposition at 0 °C.¹¹ The triamines (MesNHCH₂CH₂)₂NH and (Ar_{Cl}NHCH₂CH₂)₂NMe, where Ar_{Cl} = 2,6-Cl₂C₆H₃, were attached to Zr by an amine elimination reaction with Zr(NMe₂)₄, affording [(MesNCH₂CH₂)₂NH]Zr(NMe₂)₂ and [(Ar_{Cl}NCH₂CH₂)₂NMe]Zr(NMe₂)₂, respectively. Treatment of these Zr dimethylamide species with SiMe₃Cl affords the corresponding chloride derivatives, which upon alkylation with MeMgI or MeMgBr yields [(MesNCH₂CH₂)₂NMe]ZrMe₂ and [(Ar_{Cl}NCH₂CH₂)₂NMe]ZrMe₂.

Amine elimination and toluene elimination strategies based upon M(NR₂)₄ and M(benzyl)₄, where R = Me, Et; M = Ti, Zr, Hf, often provide suitable alternatives to conventional metathesis reactions for the preparation of electrophilic metal diamide^{5,7–47} and dibenzyl^{17,18,24,37,38,44,45,48–61} complexes featuring a variety of

bidentate and multifunctional ligands. The related amine elimination and toluene elimination reactions of H₂Ln with M(NR₂)₂Cl₂ or a M(benzyl)₂Cl₂ equivalent offer two potentially attractive routes to the corresponding metal dichloride complexes, L_nMCl₂ (eq 1 and 2). In



their patent application, researchers⁶² at Peroxid-Chemie G.m.b.H. in Germany reported that heating stoichiometric amounts of Ti(NMe₂)₂Cl₂ and (C₅Me₄H)Si(NH-t-Bu) directly affords [(C₅Me₄)SiMe₂(N-t-Bu)]TiCl₂. The analogous approach was employed by Steinhuebel and Lippard to prepare (Me₂ATI)₂TiCl₂, where Me₂ATI is *N,N'*-dimethylaminotroponimate.⁶³ Ti(NMe₂)₂Cl₂ is normally obtained by the comproportionation reaction of Ti(NMe₂)₄ and TiCl₄.⁶⁴ However, we have found that the Ti(NR₂)₂Cl₂ complexes, where R = Me, Et, are also accessible by the stoichiometric treatment of Ti(NR₂)₄ with 2 equiv of SiMe₃Cl. The Zr and Hf dibenzyl dichloride complexes, M(benzyl)₂Cl₂(Et₂O)₂, were originally prepared by treatment of an ether solution of M(benzyl)₄ with 2 equiv of HCl gas.⁶⁵ Because of their thermal instability and photosensitivity, these species must be made and handled in the dark at temperatures at or below 0 °C. Zr(benzyl)₂Cl₂(Et₂O)₂ may also be generated by deprotonation of Zr(benzyl)₄ with 2 equiv of [NEt₃H]Cl (vide infra) under similar conditions.

In this paper we report the results of our efforts to develop alternative synthetic routes based upon modified amine elimination and toluene elimination strategies for the efficient preparation of five-coordinate group 4 metal complexes featuring a tridentate diamidoamine ligand. For this purpose we employed the triamines, (MesNHCH₂CH₂)₂NR, R = H, SiMe₃. The latter triamine provided the opportunity to evaluate the stereoelectronic influence of the bulky SiMe₃ group on the M–N(amine) bond and the molecular structure. Where as the amine elimination reactions of these triamines

(21) Hughes, A. K.; Meetsma, A.; Teuben, J. H. *Organometallics* **1993**, *12*, 1936–1945.

(22) Herrmann, W. A.; Morawietz, M. J. A. *J. Organomet. Chem.* **1994**, *482*, 169–181.

(23) Diamond, G. M.; Rodewald, S.; Jordan, R. F. *Organometallics* **1995**, *14*, 5–7.

(24) Black, D. G.; Swenson, D. C.; Jordan, R. F.; Rogers, R. D. *Organometallics* **1995**, *14*, 3539–3550.

(25) Scollard, J. D.; McConville, D. H.; Vittal, J. J. *Organometallics* **1995**, *14*, 5478–5480.

(26) Carpenetti, D. W.; Kloppenburg, L.; Kupec, J. T.; Petersen, J. L. *Organometallics* **1996**, *15*, 1572–1581.

(27) Diamond, G. M.; Jordan, R. F.; Petersen, J. L. *Organometallics* **1996**, *15*, 4030–4037.

(28) Christopher, J. N.; Diamond, G. M.; Jordan, R. F.; Petersen, J. L. *Organometallics* **1996**, *15*, 4038–4044.

(29) Diamond, G. M.; Jordan, R. F.; Petersen, J. L. *Organometallics* **1996**, *15*, 4045–4053.

(30) Diamond, G. M.; Jordan, R. F.; Petersen, J. L. *J. Am. Chem. Soc.* **1996**, *118*, 8024–8033.

(31) Guérin, F.; McConville, D. H.; Vittal, J. J. *Organometallics* **1996**, *15*, 5586–5590.

(32) Christopher, J. N.; Jordan, R. F.; Petersen, J. L.; Young, V. G. *Organometallics* **1997**, *16*, 3044–3050.

(33) Kim, I.; Nishihara, Y.; Jordan, R. F.; Rogers, R. D.; Rheingold, A. L.; Yap, G. P. A. *Organometallics* **1997**, *16*, 3314–3323.

(34) Sinnema, P.-J.; van der Veen, L.; Spek, A. L.; Veldman, N.; Teuben, J. H. *Organometallics* **1997**, *16*, 4245–4247.

(35) Scollard, J. D.; McConville, D. H.; Vittal, J. J. *Organometallics* **1997**, *16*, 4415–4420.

(36) Black, D. G.; Jordan, R. F.; Rogers, R. D. *Inorg. Chem.* **1997**, *36*, 103–108.

(37) Martin, A.; Uhrhammer, R.; Gardner, T. G.; Jordan, R. F.; Rogers, R. D. *Organometallics* **1998**, *17*, 382–397.

(38) Rahim, M.; Taylor, N. J.; Xin, S.; Collins, S. *Organometallics* **1998**, *17*, 1315–1323.

(39) Leung, W.-P.; Song, F.-Q.; Zhou, Z.-Y.; Xue, F.; Mak, T. C. W. *J. Organomet. Chem.* **1999**, *575*, 232–241.

(40) Kakaliou, L.; Scanlon, W. J., IV; Qian, B.; Baek, S. W.; Smith, M. R., III; Motry, D. H. *Inorg. Chem.* **1999**, *38*, 5964–5977.

(41) Dawson, D. M.; Walker, D. A.; Thornton-Pett, M.; Bochmann, M. *J. Chem. Soc., Dalton Trans.* **2000**, 459–466.

(42) Peckham, T. J.; Nguyen, P.; Bourke, S. C.; Wang, Q.; Harrison, D. G.; Zoricak, P.; Russell, C.; Liable-Sands, L. M.; Rheingold, A. L.; Lough, A. J.; Manners, I. *Organometallics* **2001**, *20*, 3035–3043.

(43) Wang, H.; Wang, Y.; Li, H.-W.; Xie, Z. *Organometallics* **2001**, *20*, 5110–5118.

(44) Toupance, T.; Dubberley, S. R.; Rees, N. H.; Tyrrell, B. R.; Mountford, P. *Organometallics* **2002**, *21*, 1367–1382.

(45) Carpentier, J.-F.; Martin, A.; Swenson, D. C.; Jordan, R. F. *Organometallics* **2003**, *22*, 4999–5010.

(46) Braun, L. F.; Dreier, T.; Christy, M.; Petersen, J. L. *Inorg. Chem.* **2004**, *43*, 3976–3987.

(47) Tonzetich, Z. J.; Schrock, R. R.; Hock, A. S.; Müller, P. *Organometallics* **2005**, *24*, 3335–3342.

(48) Tjaden, E. B.; Swenson, D. C.; Jordan, R. F.; Petersen, J. L. *Organometallics* **1995**, *14*, 371–386.

(49) Cloke, F. G. N.; Geldbach, T. J.; Hitchcock, P. B.; Love, J. B. *J. Organomet. Chem.* **1996**, *506*, 343–345.

(50) Tsuie, B.; Swenson, D. C.; Jordan, R. F.; Petersen, J. L. *Organometallics* **1997**, *13*, 1392–1400.

(51) Tsukahara, T.; Swenson, D. C.; Jordan, R. F. *Organometallics* **1997**, *16*, 3303–3313.

(52) Chen, Y.-X.; Marks, T. J. *Organometallics* **1997**, *16*, 3649–3657.

(53) Shao, P.; Gendron, R. A. L.; Berg, D. J.; Bushnell, G. W. *Organometallics* **2000**, *19*, 509–520.

(54) Tshuva, E. Y.; Goldberg, I.; Kol, M. *J. Am. Chem. Soc.* **2000**, *122*, 10706–10707.

(55) Tshuva, E. Y.; Goldberg, I.; Kol, M.; Goldschmidt, Z. *Organometallics* **2001**, *20*, 3017–3028.

(56) Tshuva, E. Y.; Groysman, S.; Goldberg, I.; Kol, M.; Goldschmidt, Z. *Organometallics* **2002**, *21*, 662–670.

(57) Kao, S. C.; Khokhani, P. A. WO Patent Appl. 2002040550, 2002.

(58) Kettunen, M.; Vedder, C.; Schaper, F.; Leskelä, M.; Mutikainen, I.; Brintzinger, H.-H. *Organometallics* **2004**, *23*, 3800–3807.

(59) Groysman, S.; Tshuva, E. Y.; Goldberg, I.; Kol, M.; Goldschmidt, Z.; Shuster, M. *Organometallics* **2004**, *23*, 5291–5299.

(60) Segal, S.; Goldberg, I.; Kol, M. *Organometallics* **2005**, *24*, 200–202.

(61) Lowes, T. A.; Ward, B. D.; Whannel, R. A.; Dubberley, S. R.; Mountford, P. *Chem. Commun.* **2005**, 113–115.

(62) Munck, F.; Zeiss, W.; Hartmann, C.; Vogel, A.; Detig, A. (Peroxid-Chemie G.m.b.H., Germany) PCT Int. Appl. WO 9856831, 1998.

(63) Steinhuebel, D. P.; Lippard, S. J. *Inorg. Chem.* **1999**, *38*, 6225–6233.

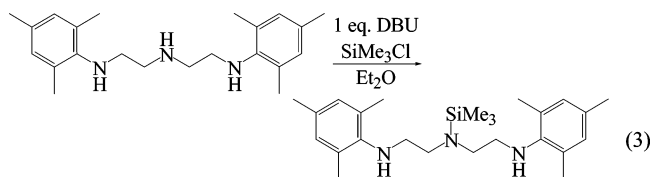
(64) Benzing, E.; Kornicker, W. *Chem. Ber.* **1961**, *94*, 2263–2267.

(65) Wengrovius, J. H.; Schrock, R. R. *J. Organomet. Chem.* **1981**, *205*, 319–327.

with $\text{Ti}(\text{NEt}_2)_2\text{Cl}_2$ afford $[(\text{MesNCH}_2\text{CH}_2)_2\text{NR}]\text{TiCl}_2$, the corresponding toluene elimination reactions of these triamines with $\text{Zr}(\text{benzyl})_2\text{Cl}_2(\text{Et}_2\text{O})_2$ yield $[(\text{MesNCH}_2\text{CH}_2)_2\text{NR}]\text{ZrCl}_2$. Specific details regarding the synthesis and structural characterization of these five-coordinate group 4 metal complexes and $[(\text{MesNCH}_2\text{CH}_2)_2\text{NH}]\text{Hf}(\text{benzyl})_2$ are described.

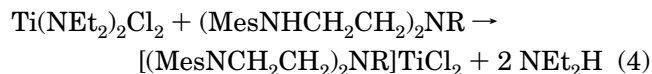
Results and Discussion

Preparation of the Triamines
 $(\text{MesNHCH}_2\text{CH}_2)_2\text{NR}$, $\text{R} = \text{H}$, SiMe_3 . The preparation of $(\text{MesNHCH}_2\text{CH}_2)_2\text{NH}$, **1**, was accomplished by the arylamination of diethylenetriamine with 2 equiv of bromomesitylene with Buchwald's $\text{Pd}_2(\text{dba})_3/\text{BINAP}$ catalyst.⁶⁶ Treatment of an ether solution of **1** with SiMe_3Cl in the presence of 1,8-diazabicyclo[5.4.0]undec-7-ene (DBU) provided a selective route for the silylation of the central amine N to afford $(\text{MesNHCH}_2\text{CH}_2)_2\text{NSiMe}_3$, **2** (eq 3). Cloke and co-workers⁶⁷ used a similar

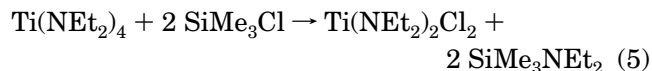


approach to prepare $(\text{Me}_3\text{SiNHCH}_2\text{CH}_2)_2\text{NSiMe}_3$ from triethylenediamine. The solution ^1H and ^{13}C NMR spectra of **2** exhibit the expected number of resonances with the protons and carbon of the trimethylsilyl substituent appearing at δ 0.11 and 0.14, respectively.

Preparation and Characterization of
 $[(\text{MesNCH}_2\text{CH}_2)_2\text{NR}]\text{TiCl}_2$, $\text{R} = \text{H}$, SiMe_3 . The five-coordinate titanium complexes $[(\text{MesNCH}_2\text{CH}_2)_2\text{NR}]\text{TiCl}_2$ ($\text{R} = \text{H}$ (**3**), SiMe_3 (**4**)) were prepared in good yields by the thermally induced amine elimination reactions of **1** and **2** with $\text{Ti}(\text{NEt}_2)_2\text{Cl}_2$ (eq 4). $\text{Ti}(\text{NEt}_2)_2\text{Cl}_2$ was



prepared by the stoichiometric reaction of $\text{Ti}(\text{NEt}_2)_4$ with 2 equiv of SiMe_3Cl (eq 5). Both compounds were isolated



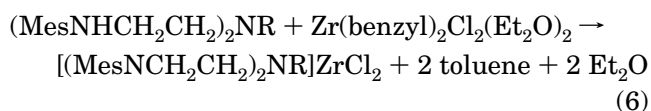
as reddish-orange solids that are moderately soluble in chloroform. The solution ^1H NMR spectrum of **3** in CDCl_3 is consistent with the presence of mirror symmetry. The *meta*-protons and the protons of the methyl substituents of the mesityl groups appear as separate singlets. The methylene protons exhibit two doublets of triplets centered at δ 3.55 and 4.19 and a more intense pseudoquartet centered at δ 3.75. The ^{13}C NMR spectrum of **3** displays the expected nine resonances for the mesityl group; the signals for the methylene carbons adjacent to the central amine nitrogen and to the amido nitrogens are observed at δ 49.2 and 60.7, respectively.

(66) Wolfe, J. P.; Wagaw, S.; Buchwald, S. L. *J. Am. Chem. Soc.* **1996**, *118*, 7215–7216.

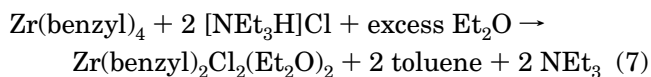
(67) Clark, H. C. S.; Cloke, F. G. N.; Hitchcock, P. B.; Love, J. B.; Wainwright, A. P. *J. Organomet. Chem.* **1995**, *501*, 333–340.

The ^1H NMR resonances of **4** are compatible with the chemical shifts observed for the proton resonances displayed by **3**. The two *meta*-protons and methyl protons of the three methyl groups of the mesityl rings are inequivalent, the methylene protons are observed as two doublets of triplets and a pseudoquartet, and the nine protons of the trimethylsilyl group give a singlet. The molecular structure of **4** was determined by an X-ray crystallographic analysis.

Preparation and Characterization of
 $[(\text{MesNCH}_2\text{CH}_2)_2\text{NR}]\text{ZrCl}_2$, $\text{R} = \text{H}$, SiMe_3 . The five-coordinate zirconium complexes $[(\text{MesNCH}_2\text{CH}_2)_2\text{NR}]\text{ZrCl}_2$ ($\text{R} = \text{H}$ (**5**), SiMe_3 (**6**)) were conveniently prepared by the reactions of $\text{Zr}(\text{benzyl})_2\text{Cl}_2(\text{Et}_2\text{O})_2$ with **1** and **2**, respectively (eq 6). The dibenzyl Zr complex,

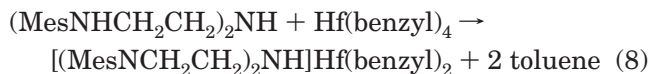


$\text{Zr}(\text{benzyl})_2\text{Cl}_2(\text{Et}_2\text{O})_2$, was prepared by protonolysis of $\text{Zr}(\text{benzyl})_4$ with 2 equiv of $[\text{NEt}_3\text{H}]\text{Cl}$ in diethyl ether (eq 7). Because of the thermal instability and light



sensitivity of $\text{Zr}(\text{benzyl})_2\text{Cl}_2(\text{Et}_2\text{O})_2$, this reaction must be performed in a darkened room while maintaining the reaction temperature at 0°C . Following replacement of diethyl ether with toluene, the corresponding triamine was added directly to the same reaction flask. Both of these toluene elimination reactions proceeded cleanly with the formation of **5** and **6**. The ^1H NMR chemical shifts of **5** are consistent with those reported by Schrock and co-workers^{9,10} for this complex. The solution ^1H and ^{13}C NMR data for **6** reflect the presence of mirror symmetry. The two *meta*-protons and the three inequivalent methyl substituents of the mesityl group display distinct singlets, and the four methylene protons afford multiplets. A singlet at δ 0.27 corresponds to the protons of the trimethylsilyl substituent. A total of 12 resonances were observed in the ^{13}C APT NMR spectrum of **6**. Four of the six aromatic resonances correspond to the four quaternary carbons of each mesityl ring with the *ipso*-carbon at δ 148.6, and the *ortho*- and *para*-carbons at δ 134.7, 133.3, and 132.8. In the gated nondecoupled ^{13}C NMR spectrum, the *meta*-carbons exhibit separate doublets δ 130.3 and 129.8 with $^1J_{\text{C-H}} = 160$. The methylene carbons appear as triplets at δ 56.8 and 52.3 with $^1J_{\text{C-H}} = 137$ and 135 Hz, respectively. The three methyl substituents within the mesityl groups give separate 1:3:3:1 quartets at δ 20.9, 20.1, and 19.4 with $^1J_{\text{C-H}} = 125$ –126 Hz. The carbon resonance of the trimethylsilyl substituent appears as a quartet at δ 0.0 with $^1J_{\text{C-H}} = 119$ Hz. The molecular structures of **5** and **6** were confirmed by X-ray crystallographic analyses.

Preparation of $[(\text{MesNCH}_2\text{CH}_2)_2\text{NH}]\text{Hf}(\text{benzyl})_2$, **7**. The reaction of $\text{Hf}(\text{benzyl})_4$ with one equivalent of **1** proceeds cleanly with the loss of 2 equiv of toluene and the formation of the Hf dibenzyl complex, $[(\text{MesNCH}_2\text{CH}_2)_2\text{NH}]\text{Hf}(\text{benzyl})_2$, **7** (eq 8).



The solution ^1H and ^{13}C NMR spectra are consistent with a mirror plane passing through the Hf, amino N, and the two benzyl methylene C atoms. The four inequivalent methylene protons within the $(\text{CH}_2)_2\text{NH}-$ $(\text{CH}_2)_2$ linkage appear as multiplets and the three inequivalent methyl groups and the two inequivalent *meta*-protons are observed as singlets. The inequivalency of the *meta* protons of the mesityl substituents was confirmed by the observation of a cross-peak in the 2D COSY NMR spectrum. The two benzyl ligands produce two distinct sets of *ortho*-, *meta*-, and *para*-proton resonances. The solution NMR spectra for the related Hf dimethyl complex, $[(\text{MesNCH}_2\text{CH}_2)_2\text{NH}]\text{HfMe}_2$, also exhibit a pair of proton and carbon resonances indicative of two inequivalent methyl ligands.⁹ The observation of the two singlets at δ 1.26 and 1.61 for the protons of the methylenes attached to Hf is further indication that the benzyl groups are inequivalent. Nine distinct carbon resonances are exhibited by the mesityl substituents, two methylene carbon resonances are displayed by the $(\text{CH}_2)_2\text{NH}(\text{CH}_2)_2$ linkage, and the two benzyl ligands provide an additional 10 resonances. The downfield resonance at δ 148.0 for the two equivalent *ipso*-C atoms of the mesityl substituents is identified by its higher intensity. The three remaining quaternary carbons of the mesityl groups are observed at δ 134.0, 134.90, and 134.93 with the three methyl carbons located at δ 19.1, 19.9, and 21.0. The two carbon resonances at δ 128.5 and 129.4 are assigned to the two inequivalent *meta*-carbons on the basis of the cross-peaks observed in the 2D COSY and HETCOR spectra. The two inequivalent methylene carbons appear as triplets centered at δ 49.1 and 57.0 with $^1J_{\text{C-H}} = 135$ Hz in the gated nondecoupled ^{13}C NMR spectrum. Finally, the 10 resonances for the two benzyl ligands were found at δ 66.0 and 74.0 with $^1J_{\text{C-H}} = 128$ Hz for the two methylene carbons bound to Hf, at δ 141.0 and 153.7 for the two *ipso*-C atoms, at δ 120.8 and 125.5 for the *para*-C atoms, and at δ 123.7, 128.6, 130.3, 130.4 for the remaining *ortho*- and *meta*-C atoms.

Discussion of the Molecular Structures. X-ray structural analyses performed on five-coordinate group 4 metal complexes featuring a dianionic tridentate diamido ligand indicate that these compounds adopt either a meridional (*mer*) or a facial (*fac*) configuration (Figure 1) within a trigonal bipyramidal framework. In the *mer* structure, the two terminal amido nitrogen donors occupy the two axial sites and the central donor atom (X) lies in the equatorial plane. The three donor atoms of the tridentate ligand in this C_{2v} -symmetric structure define a plane that bisects the L–M–L bond angle. This arrangement was reported by Schrock and co-workers for $[(\text{ArNCH}_2\text{CH}_2)_2\text{O}]\text{MR}_2$ -type complexes,^{17,18} where M = Zr or Hf, R = alkyl, Ar = 2,6-dimethylphenyl or 2,6-di-isopropylphenyl; $[(t\text{-BuN-}o\text{-C}_6\text{H}_4)_2\text{O}]\text{MMe}_2$, where M = Ti^{13,14} or Zr;¹⁴ and $[(\text{MesNCH}_2\text{CH}_2)_2\text{NMe}]\text{ZrMe}_2$.^{9,10} The corresponding $[(\text{Ar})\text{NCH}_2(\text{NC}_5\text{H}_3)\text{CH}_2\text{N}(\text{Ar})]\text{ZrCl}_2$ complexes^{31,68} that feature a planar pyridyl nitrogen donor also conform to the *mer* configuration.

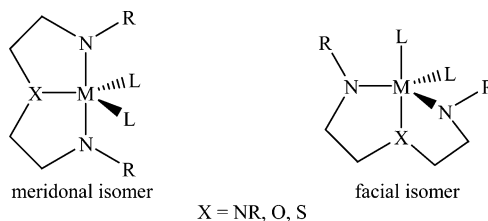


Figure 1. Structural representations of the meridional and facial stereoisomers.

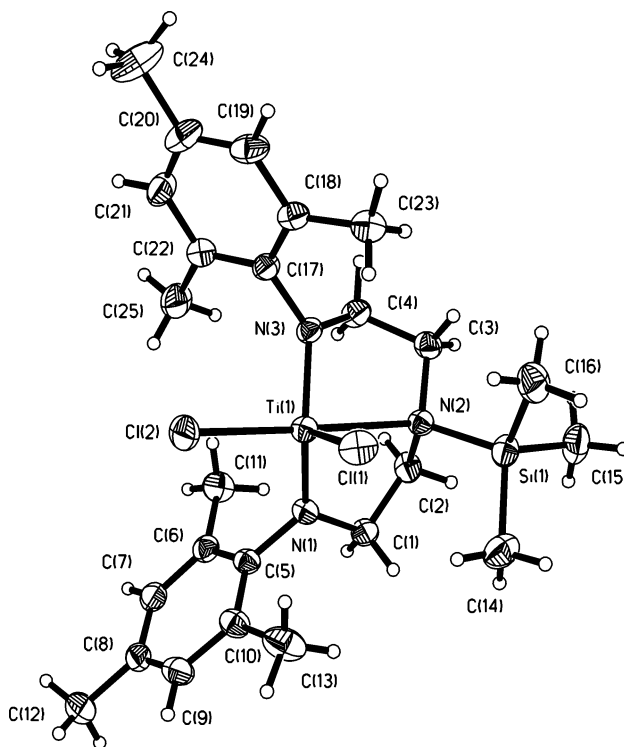


Figure 2. Perspective view of the molecular structure and the atom-labeling scheme for $[(\text{MesNCH}_2\text{CH}_2)_2\text{NSiMe}_3]\text{TiCl}_2$, **4**. The thermal ellipsoids are scaled to enclose 30% probability.

In contrast, in the C_s -symmetric *fac* structure, the two amido nitrogen donors occupy two equatorial positions and the central donor atom (X) resides in an axial position. This alternative ligand arrangement was observed for $[(\text{Me}_3\text{SiNCH}_2\text{CH}_2)_2\text{NSiMe}_3]\text{ZrCl}(\text{CH}(\text{SiMe}_3)_2)$ ⁶⁹ as well as $[(\text{ArNCH}_2\text{CH}_2)_2\text{O}]\text{Ti}(\text{benzyl})_2$ ^{17,18} and $[(\text{ArNCH}_2\text{CH}_2)_2\text{S}]\text{ZrMe}_2$,¹⁸ where Ar = 2,6-dimethylphenyl.

Perspective views of the molecular structures of $[(\text{MesNCH}_2\text{CH}_2)_2\text{NSiMe}_3]\text{TiCl}_2$ (**4**), $[(\text{MesNCH}_2\text{CH}_2)_2\text{NR}]\text{ZrCl}_2$ (R = H (**5**), SiMe₃ (**6**)), and $[(\text{MesNCH}_2\text{CH}_2)_2\text{NH}]\text{Hf}(\text{benzyl})_2$ (**7**) are depicted in Figures 2, 3, 4, and 5, respectively. The structural parameters about the central metal of **4**, **5**, and **6** indicate that these three five-coordinate complexes adopt geometries consistent with the *fac* structure. The equatorial positions of the distorted trigonal bipyramid are defined by the two amide nitrogen donor atoms and Cl(1). The respective Cl(2)–M–N(2) and Cl(1)–M–N(2) bond angles (170.23(6)° and 91.99(6)° for **4**, 169.5(2)° and 87.4(2)° for **5**, 166.41(7)° and 93.06(7)° for **6**) are consistent with Cl(2)

(68) Merkel, M.; Petersen, J. L., unpublished results.

(69) Cloke, F. G. N.; Hitchcock, P. B.; Love, J. B. *J. Chem. Soc., Dalton Trans.* **1995**, 25–30.

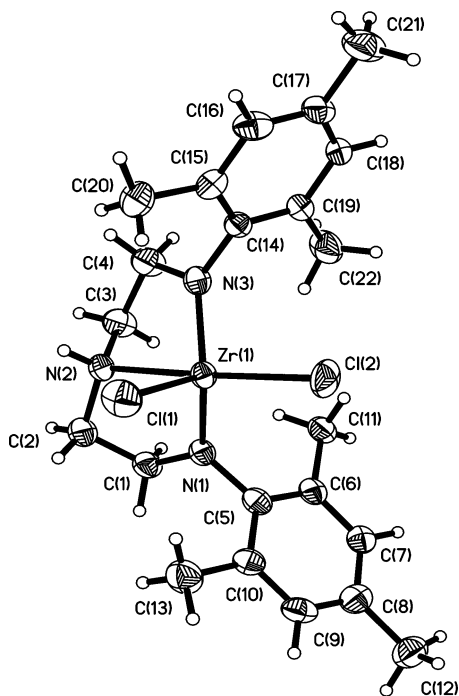


Figure 3. Perspective view of the molecular structure and the atom-labeling scheme for $[(\text{MesNCH}_2\text{CH}_2)_2\text{NH}]\text{ZrCl}_2$, **5**. The thermal ellipsoids are scaled to enclose 30% probability.

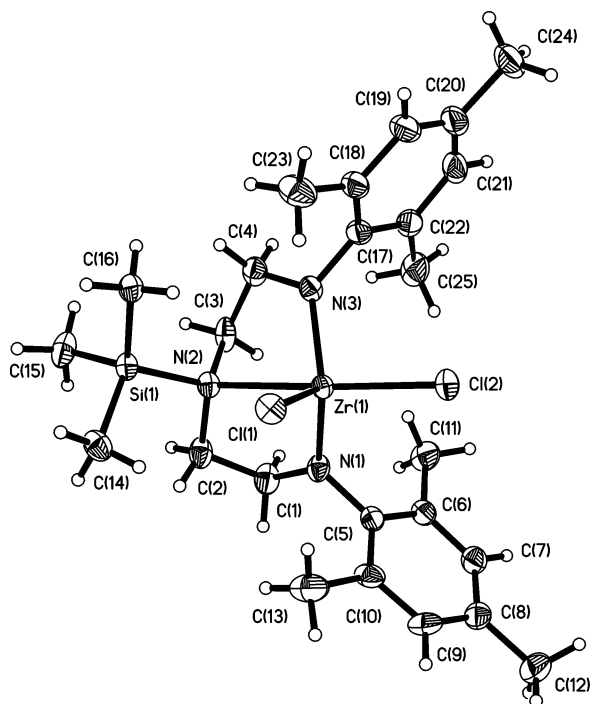


Figure 4. Perspective view of the molecular structure and the atom-labeling scheme for $[(\text{MesNCH}_2\text{CH}_2)_2\text{NSiMe}_3]\text{ZrCl}_2$, **6**. The thermal ellipsoids are scaled to enclose 30% probability.

lying trans to N(2) and Cl(1) occupying an equatorial position of a distorted trigonal bipyramid. The obtuse dihedral angles between the corresponding planes containing N(1), M, N(2) and N(2), M, N(3) of 128.0° , 131.4° , and 129.6° in **4**, **5**, and **6**, respectively, deviate substantially from the corresponding idealized dihedral angle of 180° expected for the *mer* structure but are more

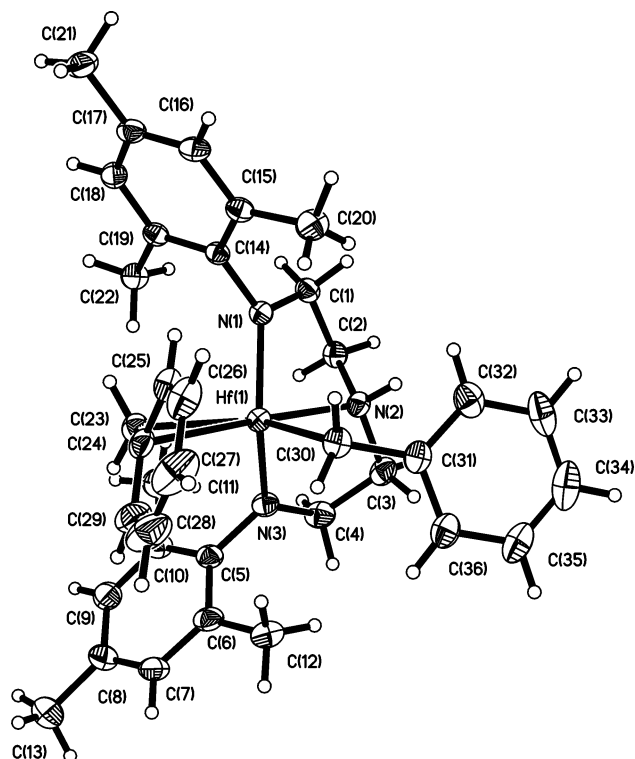


Figure 5. Perspective view of the molecular structure and the atom-labeling scheme for $[(\text{MesNCH}_2\text{CH}_2)_2\text{NH}]\text{Hf}(\text{benzyl})_2$, **7**. The thermal ellipsoids are scaled to enclose 30% probability.

similar to the 120° dihedral angle expected for the *fac* structure. Chelation of the diamidoamine ligand in these complexes produces two puckered five-membered rings with an S-shaped backbone. To reduce steric congestion about the metal atom, the two mesityl substituents of the amido nitrogen donors of **4**, **5**, and **6** are directed toward the side opposite from the equatorial chloride ligand, Cl(1), and away from the hydrogen or trimethylsilyl group at N(2). This feature is readily seen in Figure 3, which offers a view parallel to the Zr(1), Cl(1), and Cl(2) plane in **5**.

The Zr–N(amido) distances of 2.055(5) and 2.048(6) Å in **5** and 2.038(3) and 2.042(3) Å in **6** are shorter than the Zr–N(amido) distances in five-coordinate meridional d^0 Zr(IV) complexes (2.101(4) and 2.104(5) Å in $[(\text{Ar})\text{NCH}_2(\text{NC}_5\text{H}_3)\text{CH}_2\text{N}(\text{Ar})]\text{ZrMe}_2$, where Ar = 2,6-di-isopropylphenyl;³¹ 2.070(4) and 2.077(4) Å in $[(\text{Ar})\text{NCH}_2(\text{NC}_5\text{H}_3)\text{CH}_2\text{N}(\text{Ar})]\text{ZrCl}_2$, where Ar = 2,6-dimethylphenyl;⁶⁸ 2.095(4) Å in $[(\text{MesNCH}_2\text{CH}_2)_2\text{NMe}]\text{ZrMe}_2$ ^{9,10}) that also feature appreciable N(p_π)–Zr(d_π) π -bonding.⁷⁰ The shorter Zr–N(amido) bond distances observed for **5** and **6** are a consequence of the relative positions of the two amido π -donors. The N(amido)–Zr–N(amido) bond angles in **5** and **6** are ca. 120° , whereas those in $[(\text{Ar})\text{NCH}_2(\text{NC}_5\text{H}_3)\text{CH}_2\text{N}(\text{Ar})]\text{ZrCl}_2$ and $[(\text{MesNCH}_2\text{CH}_2)_2\text{NMe}]\text{ZrMe}_2$ are ca. 140° , indicating that the amido nitrogen atoms are positioned more nearly trans to each other in the *mer* structures. This arrangement places each filled nitrogen p_π -orbital in direct competition because their respective electron pairs are interacting with the same zirconium d_π -orbital.

(70) Hagen, K.; Holwill, C. J.; Rice, D. A.; Runnacles, J. D. *Inorg. Chem.* **1988**, *27*, 2032–2035.

Table 1. Crystallographic Data for 4, 5, 6, and 7

	C₂₅H₃₉Cl₂N₃SiTi, 4	C₂₅H₃₁Cl₂N₃Zr, 5	C₂₅H₃₉Cl₂N₃SiZr, 6	C₃₆H₄₅N₃Hf, 7
empirical formula	C ₂₅ H ₃₉ Cl ₂ N ₃ SiTi, 4	C ₂₅ H ₃₁ Cl ₂ N ₃ Zr, 5	C ₂₅ H ₃₉ Cl ₂ N ₃ SiZr, 6	C ₃₆ H ₄₅ N ₃ Hf, 7
fw	528.48	499.62	571.80	698.24
temperature, K	295(2)	223(2)	223(2)	223(2)
cryst syst	orthorhombic	monoclinic	orthorhombic	monoclinic
space group	<i>P</i> 2 ₁ 2 ₁ 2 ₁	<i>P</i> 2 ₁ / <i>c</i>	<i>P</i> 2 ₁ 2 ₁ 2 ₁	<i>P</i> 2 ₁ / <i>c</i>
<i>a</i> , Å	7.6772(3)	15.537(3)	8.9109(6)	16.3146(8)
<i>b</i> , Å	14.3292(6)	11.263(2)	16.1975(12)	14.6825(8)
<i>c</i> , Å	25.8800(11)	14.829(2)	19.4837(13)	14.4946(8)
β, deg		109.589(3)		113.001(1)
volume, Å ³ ; <i>Z</i>	2847.0(2), 4	2444.8(7), 4	2812.2(3), 4	3196.0(3), 4
density (calc), g/cm ³	1.233	1.357	1.351	1.451
abs coeff, cm ⁻¹	5.47	6.80	6.41	32.92
<i>F</i> (0 0 0)	1120	1032	1192	1416
cryst dimens, mm	0.09 × 0.20 × 0.41	0.10 × 0.16 × 0.36	0.12 × 0.14 × 0.20	0.17 × 0.22 × 0.32
θ range for data collection, deg	1.57 to 27.54	2.28 to 27.52	1.63–27.55	1.94–27.52
limiting indices	−9 ≤ <i>h</i> ≤ 9 −18 ≤ <i>k</i> ≤ 18 −33 ≤ <i>l</i> ≤ 33	−20 ≤ <i>h</i> ≤ 20 −14 ≤ <i>k</i> ≤ 13 −19 ≤ <i>l</i> ≤ 18	−10 ≤ <i>h</i> ≤ 11 −21 ≤ <i>k</i> ≤ 19 −24 ≤ <i>l</i> ≤ 25	−21 ≤ <i>h</i> ≤ 19 −17 ≤ <i>k</i> ≤ 18 −18 ≤ <i>l</i> ≤ 17
no. of reflns collected	20 337	16 863	20 341	22 412
no. of indep reflns	6493 (<i>R</i> _{int} = 0.0465)	5563 (<i>R</i> _{int} = 0.1156)	6393 (<i>R</i> _{int} = 0.0621)	7312 (<i>R</i> _{int} = 0.0335)
completeness, %	99.4	98.9	99.4	99.4
<i>a</i> , <i>b</i>	0.0506, 0.000	0.0728, 0.000	0.0279, 0.000	0.0267, 0.4876
refined params	298	262	298	367
GOF on <i>F</i> ²	1.020	0.968	1.010	1.022
<i>R</i> indices [<i>I</i> > 2σ(<i>I</i>)]	<i>R</i> 1 = 0.0420 w <i>R</i> 2 = 0.0960	<i>R</i> 1 = 0.0664 w <i>R</i> 2 = 0.1371	<i>R</i> 1 = 0.0438 w <i>R</i> 2 = 0.0757	<i>R</i> 1 = 0.0254 w <i>R</i> 2 = 0.0600
largest diff peak and hole, e/Å ³	0.227, −0.195	0.724, −0.636	0.379, −0.327	0.593, −0.397

Consequently, the longer Zr–N(amido) distances observed for the meridonal structures reflect a decrease in the N(p_π)–Zr(d_π) contribution to these bonds.

The corresponding Ti–N(amido) distances of 1.892(2) and 1.905(2) Å for **4** are appreciably shorter than the two Ti–N(amido) distances of 1.977(6) and 1.979(5) Å in the meridonal structure of [(Ar)NCH₂(NC₅H₃)–CH₂N(Ar)]Ti(CH₂CMe₂Ph)Br, where Ar = 2,6-dimethylphenyl,⁷¹ but are comparable to the Ti–N(amido) distances of 1.905(2) and 1.910(2) Å in the pseudo-facial complex, [(SiMe₃NCH₂CH₂)₂NSiMe₃]TiMe₂.⁶⁷ The observed variation for these Ti–N(amido) bonds can also be attributed to the relative positions of the amido π-donors. The N(amido)–Ti–N(amido) bond angles in **4** and [(SiMe₃NCH₂CH₂)₂NSiMe₃]TiMe₂ of 121.45(9)° and 124.67(9)°, respectively, are, as expected, appreciably smaller than the corresponding angle of 142.1(2)° in [(Ar)NCH₂(NC₅H₃)CH₂N(Ar)]Ti(CH₂CMe₂Ph)Br.

Whereas the amido nitrogen donors have two lone pairs for π-bonding to the electron deficient group 4 metal, the central amine nitrogen donor of the tridentate diamidoamine ligand has only one lone pair to form a dative N→Zr or N→Ti bond. As a consequence, the central M–N(amino) distances of 2.438(2), 2.361(6), and 2.475(3) Å for **4**, **5**, and **6**, respectively, are significantly longer than the corresponding M–N(amido) distances. The 0.11 Å increase in the Zr–N(amine) bond distance upon replacement of the hydrogen on the central nitrogen of **5** with the trimethylsilyl substituent in **6** reflects a decrease in the nitrogen donor strength due to the greater electron-withdrawing character of the trimethylsilyl substituent relative to hydrogen. An even more substantial elongation of the central Zr–N(amino) distance was observed for [(SiMe₃NCH₂CH₂)₂NSiMe₃]–ZrCl(CH(SiMe₃)₂).⁶⁹ In this case, the corresponding Zr–N(amino) interatomic separation of 2.770(5) Å is 0.73 Å longer than the two Zr–N(amido) distances of 2.035(5) and 2.041(5) Å.

Table 2. Selected Interatomic Distances (Å) and Bond Angles (deg) of 4, 5, and 6

	4	5	6
A. Interatomic Distances			
M–Cl(1)	2.2885(9)	2.417(2)	2.415(1)
M–Cl(2)	2.2563(10)	2.411(2)	2.402(1)
M–N(1)	1.892(2)	2.055(5)	2.038(3)
M–N(2)	2.438(2)	2.361(6)	2.475(3)
M–N(3)	1.905(2)	2.048(6)	2.042(3)
N(1)–C(1)	1.473(3)	1.472(8)	1.463(5)
N(1)–C(5)	1.450(3)	1.456(9)	1.449(5)
N(2)–C(2)	1.498(3)	1.475(9)	1.514(4)
N(2)–C(3)	1.491(3)	1.469(9)	1.503(4)
N(3)–C(4)	1.473(3)	1.470(8)	1.463(4)
N(3)–C(14)		1.449(8)	
N(3)–C(17)	1.448(3)		1.449(4)
N(2)–Si(1)	1.823(2)		1.820(3)
B. Bond Angles			
Cl(1)–M–Cl(2)	97.79(4)	103.1(1)	100.52(4)
Cl(1)–M–N(1)	116.41(7)	110.0(2)	114.82(9)
Cl(1)–M–N(2)	91.99(6)	87.4(2)	93.06(7)
Cl(1)–M–N(3)	115.03(7)	114.3(2)	115.24(9)
Cl(2)–M–N(1)	99.20(7)	104.2(2)	100.61(10)
Cl(2)–M–N(2)	170.23(6)	169.5(2)	166.41(7)
Cl(2)–M–N(3)	99.73(7)	102.8(2)	99.56(9)
N(1)–M–N(2)	76.24(8)	71.7(2)	72.95(11)
N(1)–M–N(3)	121.45(9)	120.1(2)	120.67(14)
N(2)–M–N(3)	75.96(8)	72.3(2)	74.64(11)

The covalent radius of zirconium (1.45 Å) and the ionic radius of Zr⁴⁺ (0.80 Å) are ca. 0.12–0.13 Å larger than those of titanium (1.32 Å) and Ti⁴⁺ (0.68 Å).⁷² Thus, the larger size of zirconium is expected to produce longer M–Cl and M–N bonds than titanium in similar ligand environments. A comparison of the structural data in Table 2 shows that the observed differences between the M–Cl and M–N(amido) distances for **4** and **6** are consistent with this expectation. However, the corresponding M–N(amino) bonds are more similar in magnitude. Although these long M–N(amino) bonds reflect the weaker amine nitrogen donor strength due to the trimethylsilyl substituent, an additional lengthening of

(71) Guérin, F.; McConville, D. H.; Payne, N. C. *Organometallics* **1996**, *15*, 5085–5089.

(72) Pauling, L. *The Nature of the Chemical Bond*, 3rd ed.; Cornell University Press: Ithaca, NY, 1960.

the Ti–N(2) bond in **4** arises from the more sterically crowded coordination environment about the smaller titanium metal center. A substantially weaker dative N→Ti interaction is indicated by the significantly longer Ti–N(amine) separation of 2.732(2) Å in [(SiMe₃NCH₂CH₂)₂NSiMe₃]TiMe₂.⁶⁷ The M–Cl(2) bond trans to the M–N(2) bond in **4** and in **6** is consistently shorter than the M–Cl(1) bond that lies perpendicular to the M–N(2) bond. The weaker dative bonding interaction of the neutral amino nitrogen donor in **4** and in **6** is compensated by enhanced π -donation from Cl(2) to the electrophilic metal. The noticeably larger difference, $\Delta_{\text{M-Cl}}$, between the two M–Cl distances of 0.032 Å in **4** compared to 0.013 Å in **6** provides another indication of a weaker N(2)→M dative interaction in **4** compared to **6**.

The coordination sphere about the Hf atom in **7** consists of the two sp² amido N-donors and the central sp³ amine N-donor of the tridentate diamidoamine ligand and the two benzyl ligands. The Hf–N(amido) distances of 2.050(2) and 2.074(2) Å are comparable to the Hf–N distances in d⁰ Hf-amido complexes, where there exists appreciable N(p_{π})→Hf(d_{π}) π -bonding.^{32,36,73} The lack of a π -bonding capability for the central sp³ amine N-donor results in a substantially longer Hf–N(2) distance of 2.350(3) Å. Two different coordination modes are observed for the two benzyl ligands, as indicated by the Hf–C(CH₂)–C(ipso) bond angles and the Hf⋯C(ipso) distances. The Hf–C(23)–C(24) bond angle and Hf⋯C(24) distance of 91.6(2)° and 2.741(3) Å, respectively, indicate a η^2 -benzyl interaction, whereas the Hf–C(30)–C(31) bond angle and nonbonding Hf⋯C(31) distance of 118.7(2)° and 3.283(4) Å, respectively, are consistent with a normal η^1 -benzyl bonding mode.^{24,48,74–76}

The three C atoms, C(23), C(24), and C(30), of the two benzyl ligands define a plane that essentially passes through the central Hf atom and the N(2) atom. The N(2)–Hf(1)–C(23) and N(2)–Hf(1)–C(30) bond angles of 152.2(1)° and 89.8(1)° indicate a highly unsymmetrical disposition of the two benzyl ligands within this plane. The N(2)–Hf(1)–C(24) angle of 175.6(1)° places the *ipso*-C of the η^2 -benzyl ligand trans to N(2), consistent with a *fac* structure for this compound. Chelation of the tridentate diamidoamine ligand produces two puckered five-membered chelate rings. The obtuse dihedral angle between the planes containing N(1), Hf(1), N(2) and N(2), Hf(1), N(3) of 136.9° provides further evidence of the *fac* geometry, whereby the Hf and three N atoms do not lie in the same plane. The corresponding dihedral angle between the two N, Ti, O planes in the related Ti dibenzyl complex, [(ArNCH₂CH₂)₂O]Ti(benzyl)₂, Ar = 2,6-dimethylphenyl,^{17,18} is also 137°. However, in this Ti complex both benzyl ligands are bonded in a η^1 -fashion with the Ti–C(CH₂)–C(ipso) angles being 121.0(6)° and 122.9(6)°. This difference is likely a consequence of the smaller size of Ti compared to Hf. Finally, the spatial

disposition of the methylene protons of C(30) for the η^1 -benzyl ligand sterically hinders C(24) of the η^2 -benzyl ligand from interacting more strongly with the electrophilic d⁰ Hf atom. To further reduce the steric congestion about the Hf atom, the two mesityl substituents are directed toward the same side of the molecule away from the benzyl ligands.

The orientation of the two benzyl ligands of **7** is dramatically different than observed for [(C₁₀H₆CH₂)₂-NMe]Zr(benzyl)₂,⁷⁷ which was obtained by the addition of the dilithium salt Li₂[(C₁₀H₆CH₂)₂NMe] to Zr(benzyl)₂Cl₂(Et₂O)₂. The tridentate bis(σ -aryl)amine ligand in this five-coordinate complex adopts a meridional structure with the bent wings of the two benzyl ligands pointed away from each other. In contrast, the phenyl ring of the η^2 -benzyl ligand of **7** is directed toward the η^1 -benzyl ligand. The two Zr–C(CH₂)–C(ipso) bond angles of 97.7(4)° and 110.1(4)° and Zr⋯C(ipso) distances of 2.82(1) and 3.10(1) Å in [(C₁₀H₆CH₂)₂NMe]Zr(benzyl)₂ suggest that of one of its benzyl ligands exhibits weak η^2 -character. Mountford and co-workers⁶¹ recently reported the molecular structure of [(SiMe₃NCH₂CH₂CH₂)₂NMe]Zr(benzyl)₂, which was prepared by the toluene elimination reaction of (SiMe₃NHCH₂CH₂CH₂)₂NMe with Zr(benzyl)₄. Although the diamidoamine ligand is facial in this case, both benzyl ligands exhibit η^1 -bonding, which may be a consequence of the steric bulk of the SiMe₃ substituents and the additional CH₂ link within each chelate ring.

The results of our X-ray structural analyses of **4**, **5**, **6**, and **7** reveal that these complexes adopt analogous facial structures. Their solution NMR data are consistent with the presence of C_s symmetry in solution. The S-shaped backbone of the N(CH₂)₂N(CH₂)₂N unit introduces an element of chirality in the solid-state structures of **4**, **5**, and **6**. However, the appearance of two rather than four distinct methylene carbon resonances indicates that the chemical environments of the α - and the β -methylene carbons (relative to the central amino nitrogen) are equivalent on the NMR time scale for these three compounds.

Concluding Comment. The results from this exploratory study demonstrate that Ti(NEt₂)₂Cl₂ and Zr(benzyl)₂Cl₂(Et₂O)₂ offer potentially attractive reagents for the efficient preparation of electrophilic group 4 metal dichloride complexes. The former avoids the possibility of metal reduction that sometimes occurs during conventional metathesis reactions of Ti halides and organolithio salts. These two reagents may further prove useful whenever the conversion of an intermediate organometal diamide species with SiMe₃Cl to the corresponding dichloride derivative is incomplete or proves to be problematic.

Experimental Section

Reagents. Reagent grade hydrocarbon and ethereal solvents were purified using standard methods.⁷⁸ Pentane, toluene, and THF were refluxed under nitrogen over Na/K and then transferred to storage flasks containing [(C₅H₅)₂Ti(μ -

(73) Hillhouse, G. L.; Bulls, A. R.; Santarsiero, B. D.; Bercaw, J. E. *Organometallics* **1988**, *7*, 1309–1312.

(74) Girolami, G. S.; Wilkinson, G.; Thornton-Pett, M.; Hursthouse, M. B. *J. Chem. Soc., Dalton Trans.* **1984**, 2789–2794.

(75) Latesky, S. L.; McMullen, A. K.; Niccolai, G. P.; Rothwell, I. P.; Huffman, J. C. *Organometallics* **1985**, *4*, 902–908.

(76) Pellecchia, C.; Immirzi, A.; Grassi, A.; Zambelli, A. *Organometallics* **1993**, *12*, 4473–4478.

(77) Bouwkamp, M.; van Leusen, D.; Meetsma, A.; Hessen, B. *Organometallics* **1998**, *17*, 3645–3647.

(78) Gordon, A. J.; Ford, R. A. *The Chemist's Companion*; Wiley-Interscience: New York, 1972.

$\text{Cl}_2\text{Zn}^{79}$ or $(\text{C}_5\text{H}_5)_2\text{ZrMe}_2$.^{80,81} The deuterated solvents C_6D_6 (Aldrich, 99.5%) and CDCl_3 (Aldrich, 99.8%) were dried over activated 4 Å molecular sieves prior to use, as were diethylenetriamine (Aldrich) and Et_2NH (Aldrich). $\text{TiCl}_4(\text{THF})_2$,⁸² $\text{Zr}(\text{benzyl})_4$,⁸³ and $\text{Hf}(\text{benzyl})_4$ ⁸³ were prepared by literature procedures. The workup procedure used for $(\text{MesNHCH}_2\text{CH}_2)_2\text{NH}$ was modified from the large-scale preparation originally described by Schrock and co-workers.⁹ $[\text{NET}_3\text{H}]\text{Cl}$ was prepared by the stoichiometric addition of HCl to a pentane solution of NET_3 . LiNET_2 was prepared by treatment of a pentane solution of NET_2H with 1 equiv of $n\text{-BuLi}$. TiCl_4 (Aldrich), ZrCl_4 (Aldrich), HfCl_4 (Aldrich), $n\text{-BuLi}$ (Aldrich, 1.6 M in hexanes), HCl (Matheson), NET_2H (Aldrich), NET_3 (Aldrich), SiMe_3Cl (Aldrich), 2-bromomesitylene (Aldrich), Na-O-t-Bu (Acros), $\text{Pd}_2(\text{dba})_3\cdot\text{CHCl}_3$ (Strem Chemicals), *rac*-BINAP (Strem Chemicals), and 1,8-diazabicyclo[5.4.0]undec-7-ene (DBU, Aldrich) were used without further purification.

General Considerations. All syntheses and manipulations were carried out on a double-manifold, high-vacuum line or in a Vacuum Atmospheres glovebox equipped with an HE-493 Dri-Train. Reactions were typically carried out in pressure-equalizing filter-frits equipped with high-vacuum Teflon stopcocks and Solv-seal joints. Nitrogen was purified by passage over reduced BTS catalysts and activated 4 Å molecular sieves. All glassware was thoroughly oven-dried and/or flame-dried under vacuum prior to use. NMR sample tubes were sealed under approximately 500 Torr of nitrogen. ^1H and ^{13}C NMR spectra were measured on a JEOL GX-270 or Eclipse 270 FT-NMR spectrometer. The ^1H chemical shifts are referenced to the residual proton peak of benzene- d_6 (δ 7.15) or chloroform- d_1 (δ 7.24); the ^{13}C resonances are referenced to the central carbon peak of benzene- d_6 (δ 128.0) or chloroform- d_1 (δ 77.0). Elemental analyses were performed by Complete Analysis Laboratories Inc., Parsippany, NJ.

Preparation of $\text{Ti}(\text{NET}_2)_4$. To a 100 mL Solv-seal flask equipped with a sidearm was added 1.470 g (18.6 mmol) of freshly prepared LiNET_2 . A 1.515 g (4.54 mmol) sample of $\text{TiCl}_4(\text{THF})_2$ was added to the sidearm. After the addition of dry toluene (35 mL), the $\text{TiCl}_4(\text{THF})_2$ was added in small increments. The reaction mixture was stirred overnight at room temperature and then heated at 100 °C for several hours. The toluene was replaced by 40 mL of pentane. The yellow solution was filtered and the product extracted before the solvent was removed. The brownish-red oily product (1.42 g, 92.6% yield) was dried under vacuum. The ^1H NMR spectrum indicated the product was clean. ^1H NMR (C_6D_6): δ 3.57 (q, CH_2), 1.10 (t, CH_3). $^{13}\text{C}\{^1\text{H}\}$ NMR (C_6D_6): δ 45.3 (CH_2), 15.6 (CH_3).

Preparation of $\text{Ti}(\text{NET}_2)_2\text{Cl}_2$. Toluene (30 mL) and 1.10 mL (8.67 mmol) of SiMe_3Cl were vacuum transferred into a 100 mL Solv-seal flask containing 1.349 g (4.01 mmol) of $\text{Ti}(\text{NET}_2)_4$. The reaction mixture was placed under a nitrogen atmosphere and then heated at 60 °C for 60 h. The toluene was replaced by 40 mL of pentane. The solution was filtered and the solvent was removed to afford a reddish oil (0.977 g, 92.6% yield) after removal of the volatile solvents under vacuum. The ^1H NMR spectrum indicated clean formation of the desired product. ^1H NMR (C_6D_6): δ 3.55 (q, CH_2), 0.87 (t, CH_3). $^{13}\text{C}\{^1\text{H}\}$ NMR (C_6D_6): δ 47.1 (CH_2), 14.1 (CH_3).

Preparation of $(\text{MesNHCH}_2\text{CH}_2)_2\text{NH}$, **1.** To a 100 mL Solv-seal flask were added 1.03 g (9.98 mmol) of diethylenetriamine, 4.00 g (20.1 mmol) of 2-bromomesitylene, 2.50 g

(26.0 mmol) of Na-O-t-Bu , 0.0211 g (0.0204 mmol) of $\text{Pd}_2(\text{dba})_3\cdot\text{CHCl}_3$, and 0.0379 g (0.0608 mmol) of *rac*-BINAP. Toluene (40 mL) was added via vacuum distillation. The reaction mixture was placed under a nitrogen atmosphere and heated to 100–120 °C for 40 h. The reaction mixture was cooled to room temperature and filtered. The product was extracted and the toluene removed, leaving a dark reddish solid. Pentane (30 mL) was added via vacuum distillation. The solution was filtered and the solvent removed, leaving a dark oily product. The oil was frozen by submersion of the reaction flask in liquid nitrogen. The product remained as a reddish solid after the liquid nitrogen was removed, and the flask was warmed to ambient temperature. The product (3.11 g, 91.7% yield) was dried under vacuum. ^1H NMR (CDCl_3): δ 6.81 (s, *meta*-H, 4H), 3.39 (t, NH, 2H), 3.03 (m, CH_2 , 4H), 2.83 (m, CH_2 , 4H), 2.26 (s, *ortho*-Me, 12H), 2.21 (s, *para*-Me, 6H). Gated nondecoupled ^{13}C NMR (CDCl_3) (mult., $^1J_{\text{C-H}}$ in Hz): δ 143.6 (s, *ipso*-C), 131.2 (s, *para*-C), 129.7 (s, *ortho*-C), 129.4 (d, *meta*-CH, 158), 50.0 (t, CH_2 , 133), 48.4 (t, CH_2 , 136), 20.5 (q, *para*-Me, 125), 18.3 (q, *ortho*-Me, 126).

Preparation of $(\text{MesNHCH}_2\text{CH}_2)_2\text{NSiMe}_3$, **2.** To a 100 mL Solv-seal flask equipped with a sidearm was added 1.236 g (8.12 mmol) of DBU. To the sidearm was added 2.769 g (8.16 mmol) of **1**. Diethyl ether (35 mL) and 1.1 mL (8.67 mmol) of SiMe_3Cl were added via vacuum distillation. The DBU/ $\text{SiMe}_3\text{Cl}/\text{Et}_2\text{O}$ solution was placed under a nitrogen atmosphere and stirred at room temperature for 1 h, immediately forming a white solid. The triamine was added in small increments. The reaction mixture was stirred overnight at room temperature. The solution was filtered, the product extracted with pentane, and the solvent removed. The oily product (3.11 g, 92.6%) was dried under vacuum to remove any volatiles. The NMR spectra indicated the isolated product was sufficiently pure to use. ^1H NMR (CDCl_3): δ 6.79 (s, *meta*-H, 4H), 2.97 (m, CH_2 , 8H), 2.22 (s, *ortho*-Me, 12H), 2.21 (s, *para*-Me, 6H), 0.11 (s, SiMe_3 , 9H). $^{13}\text{C}\{^1\text{H}\}$ NMR (CDCl_3): δ 143.6 (*ipso*-C), 130.9 (*para*-C), 129.4 (*meta*-CH), 129.1 (*ortho*-C), 47.1, 46.5 (CH_2), 20.5 (*para*-Me), 18.4 (*ortho*-Me), 0.14 (SiMe_3).

$(\text{MesNCH}_2\text{CH}_2)_2\text{NH}\text{TiCl}_2$, **3.** To a 100 mL Solv-seal flask were added 2.175 g (8.26 mmol) of $\text{Ti}(\text{NET}_2)_2\text{Cl}_2$, 2.804 g (8.26 mmol) of **1**, and 45 mL of toluene. The reaction mixture was heated at 100 °C overnight under a nitrogen flush for 48 h. The toluene was removed and the product residue was washed with pentane (3 × 25 mL) to extract any soluble impurities. Removal of the volatiles left 3.464 g (91.8% yield) of a reddish orange powder. ^1H NMR (CDCl_3) (mult., $J_{\text{H-H}}$ in Hz): δ 6.85, 6.83 (s, *meta*-H, 4H), 4.19 (dt, CH_2 , 13.8, 6.0, 2H), 3.75 (pseudo-q, CH_2 , 6.0, 6.1, 4H), 3.55 (dt, CH_2 , 13.8, 6.1, 2H), 2.36, 2.27, 2.21 (s, *ortho*- and *para*-Me, 18H). $^{13}\text{C}\{^1\text{H}\}$ NMR (CDCl_3): δ 135.7 (*ipso*-C), 131.9 (*para*-C), 129.7, 129.3 (*ortho*-C), 129.25, 129.2 (*meta*-CH), 60.7, 49.2 (CH_2), 20.8 (*para*-Me), 18.9, 18.8 (*ortho*-Me). Anal. Calcd for $\text{C}_{22}\text{H}_{31}\text{N}_3\text{Cl}_2\text{Ti}$: C, 57.91; H, 6.85; N, 9.21. Found: C, 56.98; H, 6.96; N, 8.92. The low carbon percentage may reflect Ti carbide formation during the combustion analysis.

Preparation of $(\text{MesNCH}_2\text{CH}_2)_2\text{NSiMe}_3\text{TiCl}_2$, **4.** Toluene (40 mL) was added to a 100 mL Solv-seal flask containing 1.736 g (6.60 mmol) of $\text{Ti}(\text{NET}_2)_2\text{Cl}_2$ and 2.716 g (6.60 mmol) of **2**. The reaction was stirred overnight while heating to 100 °C under a nitrogen flush. After removal of the volatiles, the product was washed with pentane (3 × 30 mL), leaving 2.047 g (58.7% yield) of a reddish-orange powder. ^1H NMR (CDCl_3) (mult., $J_{\text{H-H}}$ in Hz): δ 6.85, 6.83 (s, *meta*-H, 4H), 4.19 (dt, CH_2 , 13.8, 5.8, 2H), 3.75 (pseudo-q, CH_2 , 6.0, 5.8, 4H), 3.57 (dt, CH_2 , 13.8, 6.0, 2H), 2.36, 2.27, 2.22 (s, *ortho*- and *para*-Me, 18H), 0.52 (s, SiMe_3). $^{13}\text{C}\{^1\text{H}\}$ NMR (CDCl_3): δ not obsd (*ipso*-, *ortho*-, and *para*-C), 129.3, 129.2 (*meta*-CH), 61.3, 52.7 (CH_2), 20.8 (*para*-Me), 19.5, 18.8 (*ortho*-Me), 0.5 (SiMe_3). Anal. Calcd for $\text{C}_{25}\text{H}_{39}\text{N}_3\text{Cl}_2\text{SiTi}$: C, 56.82; H, 7.44; N, 7.95. Found: C, 56.74; H, 7.60; N, 8.16.

(79) Sekutowski, D. G.; Stucky, G. D. *Inorg. Chem.* **1975**, *14*, 2192–2199.

(80) Samuel, E.; Rausch, M. D. *J. Am. Chem. Soc.* **1973**, *95*, 6263–6267.

(81) Hunter, W. E.; Hrcncir, D. C.; Vann Bynum, R.; Penttila, R. A.; Atwood, J. L. *Organometallics* **1993**, *2*, 750–755.

(82) Manzer, L. E. *Inorg. Synth.* **1982**, *21*, 135–136.

(83) Zucchini, U.; Albizzati, E.; Giannini, U. *J. Organomet. Chem.* **1971**, *26*, 357–372.

Preparation of [(MesNCH₂CH₂)₂NH]ZrCl₂, **5.** To a 250 mL round-bottom flask equipped with two sidearms was added 3.887 g (8.53 mmol) of Zr(benzyl)₄. To one sidearm was added 2.348 g (17.06 mmol) of [NEt₃H]Cl. To the other sidearm was added 2.896 g (8.53 mmol) of **1**. Diethyl ether (ca. 60 mL) was added via vacuum distillation. The reaction was stirred at 0 °C while the [NEt₃H]Cl was added in small increments. After the volatiles were removed, toluene (75 mL) was added. The reaction mixture was stirred at 0 °C while **1** was added in small increments. The reaction was then warmed to room temperature and stirred overnight. The solution was filtered and the product extracted before the toluene was removed. The product residue was then washed with 45 mL of pentane to remove any soluble impurities. The remaining light tan solid (3.745 g, 87.9% yield) was dried in vacuo. The ¹H NMR spectrum confirmed the formation of **5** as the only product. ¹H NMR (CDCl₃): δ 6.87 (s, *meta*-H, 4H), 3.86, 3.55, 3.45 (m, CH₂, 8H), 2.37, 2.32, 2.22 (s, *ortho*- and *para*-Me). Gated nondecoupled ¹³C NMR (CDCl₃) (mult., ¹J_{C-H} in Hz): δ 145.0 (s, *ipso*-C), 135.3, 134.1, 133.7 (s, *ortho*- and *para*-C), 129.6, 129.5 (d, *meta*-CH, 161), 56.8 (t, CH₂, 137), 49.2 (t, CH₂, 134), 20.9 (q, *para*-Me, 126), 18.8, 18.7 (q, *ortho*-Me, 125). Anal. Calcd for C₂₂H₃₁N₃Cl₂Zr: C, 52.89; H, 6.25; N, 8.41. Found: C, 52.78; H, 6.52; N, 8.15.

Preparation of [(MesNCH₂CH₂)₂NSiMe₃]ZrCl₂, **6.** To a 250 mL round-bottom flask equipped with two sidearms was added 3.652 g (8.01 mmol) of Zr(benzyl)₄. To one sidearm was added 2.206 g (16.03 mmol) of [NEt₃H]Cl. To the other sidearm was added 3.299 g (8.01 mmol) of **2**. Diethyl ether (60 mL) was added via vacuum distillation. The reaction was stirred at 0 °C while the [NEt₃H]Cl was added in small increments. The volatiles were then removed and toluene (65 mL) was added. The reaction was stirred at 0 °C while **2** was added in small increments. The reaction was then warmed to room temperature and stirred overnight. The solution was filtered and the toluene removed. The product was then washed with 40 mL of pentane. The off-white solid (3.394 g, 74.1% yield) was dried under vacuum. The ¹H NMR spectrum confirmed the formation of **6** as the only product. ¹H NMR (C₆D₆): δ 6.90, 6.80 (s, *meta*-H, 4H), 3.63, 3.03, 2.84, 2.68 (m, CH₂, 8H), 2.57, 2.48, 2.12 (s, *ortho*- and *para*-Me, 18H), 0.27 (s, SiMe₃, 9H). Gated nondecoupled ¹³C NMR (C₆D₆) (mult., ¹J_{C-H} in Hz): δ 148.6 (s, *ipso*-C), 134.7, 133.3, 132.8 (s, *ortho*- and *para*-C), 130.3, 129.8 (d, *meta*-CH, 160), 56.8 (t, CH₂, 137), 52.3 (t, CH₂, 135), 20.9 (q, *para*-Me, 125), 20.1, 19.4 (q, *ortho*-Me, 126), 0.0 (q, SiMe₃, 119). Anal. Calcd for C₂₅H₃₉N₃Cl₂SiZr: C, 52.51; H, 6.87; N, 7.35. Found: C, 52.29; H, 7.07; N, 7.27.

Preparation of [(MesNCH₂CH₂)₂NH]Hf(benzyl)₂, **7.** To a 100 mL Solv-seal flask was added 170 mg (0.5 mmol) of **1** and 272 mg (0.5 mmol) of Hf(benzyl)₄. Approximately 20 mL of pentane was added via vacuum distillation, and the solution was allowed to stir overnight. The pentane was removed slowly into a liquid N₂ filled trap, leaving an off-white solid, which was washed with cold pentane and dried under high vacuum. Slow removal of solvent from a saturated diethyl ether solution provided suitable crystals for X-ray crystallographic analysis. The isolated yield was 286 mg (82% yield). ¹H NMR (C₆D₆): δ 7.15 (m, aryl-H, 2H), 7.04 (t, *para*-H, 1H), 6.96 (d, *meta*-H, 2H), 6.92 (m, aryl-H, 2H), 6.90 (m, aryl-H, 2H), 6.85 (m, aryl-H, 2H), 6.76 (t, *para*-H, 1H), 6.15 (d, *meta*-H, 2H), 3.39, 3.16, 2.36, 2.20 (m, NCH₂, 8H), 2.55, 2.39, 2.19 (s, *ortho*- and *para*-Me, 18H), 1.61, 1.26 (s, HfCH₂, 4H). ¹³C NMR (C₆D₆) (mult., ¹J_{C-H} in Hz): δ 148.0 (*ipso*-C, Mes), 153.7, 141.0 (*ipso*-C, benzyl), 134.93, 134.90, 134.0 (*ortho*- and *para*-C), 130.4, 130.3, 129.4, 128.6, 128.5, 125.5, 123.7, 120.8, (d, aryl-CH, average 158), 74.0, 66.0, (t, HfCH₂, 128), 57.0, 49.1 (t, NCH₂, 135), 21.0 (q, *para*-Me, 125), 19.9, 19.1 (q, *ortho*-Me, 125). 2D HETCOR NMR (C₆D₆): δ 7.15/128.6 (aryl-CH), 7.04/125.5 (*para*-CH, benzyl), 6.96/129.4 (*meta*-CH, Mes), 6.92/130.4 (aryl-CH), 6.90/130.3 (aryl-CH), 6.85/123.7 (aryl-CH), 6.76/120.8 (*para*-CH, benzyl), 6.15/128.5 (*meta*-CH, Mes), 3.39, 3.16/57.0; 2.36, 2.20/

Table 3. Selected Interatomic Distances (Å) and Bond Angles (deg) for [(MesNCH₂CH₂)₂NH]Hf(benzyl)₂, **7**

A. Interatomic Distances			
Hf(1)–N(1)	2.074(2)	Hf(1)–N(2)	2.350(3)
Hf(1)–N(3)	2.050(2)	Hf(1)–C(23)	2.282(3)
Hf(1)–C(30)	2.301(3)	Hf(1)–C(24)	2.741(3)
N(1)–C(1)	1.470(4)	N(1)–C(14)	1.440(3)
N(2)–C(2)	1.466(3)	N(2)–C(3)	1.473(4)
N(3)–C(4)	1.465(4)	N(3)–C(5)	1.448(4)
C(1)–C(2)	1.509(4)	C(3)–C(4)	1.514(4)
C(23)–C(24)	1.455(4)	C(30)–C(31)	1.483(4)
B. Bond Angles			
N(1)–Hf(1)–N(2)	72.3(1)	N(1)–Hf(1)–N(3)	124.3(1)
N(2)–Hf(1)–N(3)	71.6(1)	N(1)–Hf(1)–C(23)	97.0(1)
N(1)–Hf(1)–C(24)	110.1(1)	N(1)–Hf(1)–C(30)	112.3(1)
N(2)–Hf(1)–C(23)	152.2(1)	N(2)–Hf(1)–C(24)	175.6(1)
N(2)–Hf(1)–C(30)	89.8(1)	N(3)–Hf(1)–C(23)	95.9(1)
N(3)–Hf(1)–C(24)	109.1(1)	N(3)–Hf(1)–C(30)	108.5(1)
C(23)–Hf(1)–C(24)	32.1(1)	C(23)–Hf(1)–C(30)	117.9(1)
C(1)–N(1)–Hf(1)	122.3(2)	C(5)–N(3)–Hf(1)	122.5(2)
C(1)–N(1)–C(14)	110.6(2)	C(4)–N(3)–C(5)	111.0(2)
C(14)–N(1)–Hf(1)	127.1(2)	C(4)–N(3)–Hf(1)	126.2(2)
C(2)–N(2)–Hf(1)	105.4(2)	C(3)–N(2)–Hf(1)	112.0(2)
C(2)–N(2)–C(3)	114.4(2)	N(1)–C(1)–C(2)	108.0(2)
C(1)–C(2)–N(2)	107.1(2)	N(2)–C(3)–C(4)	107.6(2)
C(3)–C(4)–N(3)	108.6(2)	C(24)–C(23)–Hf(1)	91.6(2)
C(31)–C(30)–Hf(1)	118.7(2)		

49.1 (NCH₂), 2.55/19.9, 2.39/19.1, 2.19/21.0 (*ortho*- and *para*-Me), 1.61/74.0 (HfCH₂), 1.26/66.0 (HfCH₂). Anal. Calcd for C₃₆H₄₅N₃Hf: C, 61.93; H, 6.50; N, 6.02. Found: C, 61.89; H, 6.52; N, 6.22.

Description of the X-ray Structural Analyses. The X-ray structural analyses of **4**, **5**, **6**, and **7** were performed by using the same general procedures. Suitable crystals of **4–7** for the structural and elemental analyses were grown by slow removal of diethyl ether from saturated solutions. Each crystal was coated with the perfluoropolyether PFO-XR75 (Lancaster) and sealed under nitrogen in a glass capillary. Each sample was optically aligned on the four-circle of a Siemens P4 diffractometer equipped with a graphite monochromatic crystal, a Mo K α radiation source ($\lambda = 0.71073$ Å), and a SMART CCD detector held at 5.054 cm from the crystal. The samples of **5**, **6**, and **7** were cooled to -50 °C by the nitrogen cold stream provided by a LT-2 low-temperature attachment. Four sets of 20 frames each were collected using the ω scan method with a 10 s exposure time. Integration of these frames followed by reflection indexing and least-squares refinement produced the crystal orientation matrix and preliminary lattice parameters.

Data acquisition consisted of the measurement of a total of 1650 frames in five different runs covering a hemisphere of data. The program SMART (version 5.6)⁸⁴ was used for diffractometer control, frame scans, indexing, orientation matrix calculations, least-squares refinement of cell parameters, and the data collection. All 1650 crystallographic raw data frames were read by the program SAINT (version 5/6.0)⁸⁴ and integrated using 3D profiling algorithms. An absorption correction was applied using the SADABS routine available in SAINT. The data were corrected for Lorentz and polarization effects as well as any crystal decay. The linear absorption coefficient, atomic scattering factors, and anomalous dispersion corrections were calculated from values from the International Tables for X-ray Crystallography.⁸⁵

Initial coordinates for all of the non-hydrogen atoms were determined by a combination of direct methods and difference Fourier methods with the use of SHELXTL 6.1.⁸⁶ Idealized

(84) SMART, SAINT, and XPREP programs are part of the Bruker crystallographic software package for single-crystal data collection, reduction, and preparation.

(85) International Tables for X-ray Crystallography; Kynoch Press: Birmingham (Present distributor, D. Reidel, Dordrecht), 1974; Vol. IV, p 55.

positions for the hydrogen atoms were included as fixed contributions using a riding model with isotropic temperature factors set at 1.2 (aromatic and methylene protons) or 1.5 (methyl protons) times that of the adjacent carbon. The positions of the methyl hydrogen atoms were optimized by a rigid rotating group refinement with idealized tetrahedral angles. Full-matrix least-squares refinement, based upon the minimization of $\sum w_i |F_o^2 - F_c^2|^2$, with $w_i^{-1} = [\sigma^2 (F_o^2) + (aP)^2 + bP]$, where $P = (\text{Max}(F_o^2, 0) + 2F_c^2)/3$, converged to give final discrepancy indices⁸⁷ tabulated in Table 1. Pertinent interatomic distances and bond angles for the molecular structures of the dichloride complexes **4**, **5**, and **6** and the dibenzyl complex **7** are provided in Tables 2 and 3, respectively.

Acknowledgment. Financial support for this research was provided by the donors of the Petroleum Research Fund, administered by the American Chemi-

(86) Sheldrick, G. M. *SHELXTL6.1*, Crystallographic software package; Bruker AXS, Inc.: Madison, WI, 2000.

cal Society. J.L.P. gratefully acknowledges the financial support provided by the Eberly College of Arts and Sciences and the C. Eugene Bennett Department of Chemistry and the unrestricted research funds provided by Union Carbide Corporation and The Dow Chemical Company to acquire a SMART CCD detector for the Siemens P4 X-ray diffractometer at West Virginia University.

Supporting Information Available: Complete tables of the results from the X-ray structural analyses performed on compounds **4**–**7**. This material is available free of charge via the Internet at <http://pubs.acs.org>.

OM0580349

(87) The equations for the *R*-factors are $R_1 = \sum(|F_o| - |F_c|)/\sum|F_o|$ and $wR_2 = [\sum[w(F_o^2 - F_c^2)^2]/\sum w[F_o^2]^2]^{1/2}$. The expression for the "goodness-of-fit" is $\text{GOF} = [\sum[w(F_o^2 - F_c^2)^2]/(n-p)]^{1/2}$, where *n* is the number of reflections and *p* is the total number of parameters that were varied during the last refinement cycle.